$\alpha(Z\alpha)^2$ Vacuum-Polarization Correction in Muonic Atoms*

Thomas L. Bell†‡
The Enrico Fermi Institute, and the Department of Physics, The University of Chicago, Chicago, Illinois 60637
(Received 21 December 1972)

We use the Laplace transform obtained by Wichmann and Kroll for the vacuum-polarization charge density of order $(Z\alpha)^3$ induced by a point nucleus to determine the first few terms in the expansion of the charge density for small distances from the nucleus. The result is used to estimate the effect of the polarization charge near the nucleus on the muonic x rays studied experimentally by Dixit *et al.* The effect is found to be somewhat smaller than an earlier estimate, and the discrepancy between theory and experiment is slightly reduced, but the discrepancy remains large for the high-Z muonic atoms, as much as three or four standard devitations in lead and barium.

I. INTRODUCTION

Quantum electrodynamics makes precise statements about the behavior of the muon when it enters into association with an atomic nucleus to form a muonic atom. To the extent that its weak interactions can be ignored, the muon is treated as no more than a weightier brother to the electron, differing in its behavior only insofar as can be explained by its larger mass. Except for one case, there is no disagreement between experiment and the predictions based on this treatment of the muon, not only for muonic atoms, but in all situations involving muons in which weak interactions can be neglected.[1]

The one exception is the experiment of Dixit *et al.*[2] They reported that very precise measurements of the energies of x rays emitted by many different muonic atoms fell consistently below the theoretical predictions, often by many standard deviations. They had concentrated on transitions of the muonic atoms that should be relatively insensitive to nuclear-structure effects, and yet occur far enough within the interior of the atom so that the influence of the surrounding electrons can be easily taken into account. For this judicious selection of x-ray lines the muonic atoms may be treated as essentially hydrogenlike and their transition energies determined by the well-developed methods for handling such atoms. The only sources of ambiguity—nuclear structure and the electronic environment—are reduced to perturbations that are believed to be known to within the accuracy of the experiment.

If the experiment is correct, then the discrepancy is either due to a mistake in the application of the theory for the transition energies of the muonic atoms or to an anomalous interaction of the muon. It would be premature to introduce a muonic anomaly before trying to see if the accepted theory cannot account for the discrepancy, and it was in pursuing such an explanation that the work described here evolved.

Since the muonic atoms are approximately hydrogenlike, their energy levels are nearly those given by the solutions to the Dirac equation for a point nucleus. Perturbations to these energies arise from radiative corrections, the finite size and the structure of the nucleus, and interaction with the atomic electrons.

Among the radiative corrections are those that arise from the polarization of the vacuum by the nuclear charge. The diagrams representing this effect that contribute signficant corrections are shown in Fig. 1. The nucleus is so heavy that it may be treated as a fixed source in computing these corrections. The dangling photon line represents the Coulomb interaction of the muon (not shown) with the polarization charge induced in the

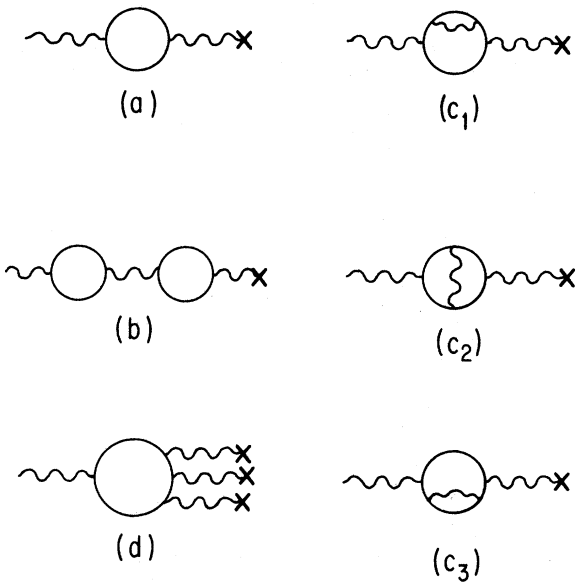

FIG. 1. Vacuum-polarization diagrams significant in affecting transition energies in muonic atoms. The × represents the nuclear charge, and the fermion is an electron.

vacuum by the nucleus.

The diagram in Fig. 1(d) represents the distortion of the polarization charge distribution due to the continuing influence of the nuclear charge on it. This diagram, and the corresponding diagrams with more and more photon lines attached between the nucleus and the electron loop, will be considered here. Its effect has not been significant in experiments with electronic atoms, because it is of order $(Z\alpha/\pi)^2$ in size relative to the first-order vacuum-polarization effect [Fig. 1(a)]; in hydrogen this is minuscule, and in heavier elements it is small compared with the uncertainties in handling the many-electron atom. But the muon, because it is so much heavier, can orbit close to the nucleus, where the influence of the atomic electrons is small compared with that of the unscreened nuclear charge nearby, and in heavy muonic atoms the effect of the diagram is neither small relative to present-day experiments nor buried in the many-body problem.

This diagram may be imagined to represent the nucleus pulling the virtual electrons in closer to itself, increasing the negative charge within the orbit of the muon, so that in making a transition to a lower orbit the muon must work against the repulsion of the additional charge, and the energy of the transition is reduced. The actual polarization charge distribution implied by the diagram is extremely difficult to calculate with the usual momentum-space methods that serve in evaluating all the other diagrams, and to our knowledge such a calculation has not yet been carried through. However, Wichmann and Kroll[3] succeeded in finding the Laplace transform of the charge density by means of a very clever observation. They noted that the sum of all the diagrams with a single electron loop attached to the nuclear charge with any number of photon lines, including the ones in Figs. 1(a) and 1(d), could be represented by the single diagram with the electron loop replaced by a loop representing the Green's function for propagation of the electron in the presence of the Coulomb field of the nucleus. By working with this Green's function instead of an individual diagram, they were able to obtain the Laplace transform of the polarization charge density, and by expanding their result in powers of $Z\alpha$ they could regain the charge density due to the corresponding order in perturbation theory. The term linear in $Z\alpha$ agreed with the well-known perturbation calculation based on the diagram in Fig. 1(a), and the third-order term in $Z\alpha$ yielded the asymptotic behavior for large distances known from the Euler–Heisenberg Lagrangian for weak electromagnetic fields.

Since it is its Laplace transform and not the charge density itself that is obtained, the spatial distribution of the charge density can only be known to the extent that the transform can be inverted. But it is not obvious how to do this analytically, so that the only information known about the behavior of the charge density is that which can be derived from the asymptotic behavior of the Laplace transform. Wichmann and Kroll pursued their calculation far enough to determine the charge density at the nucleus and very far away from the nucleus, and some characteristics about the average behavior of the charge density. It will be useful for future reference to review some of their results in Sec. II. In Sec. III additional information about the behavior of the polarization charge near the nucleus is obtained from its Laplace transform and applied to the muonic atoms. Its effect is seen to be smaller than a previous estimate, and the discrepancy between theory and experiment is slightly reduced, but the disagreement remains large for heavy muonic atoms.

II. REVIEW OF SOME RESULTS FOR DIAGRAM IN FIGURE 1(d)

In Eq. (WK51) (the prefix "WK" will be used to identify equations from Ref. 3), Wichmann and Kroll define the Laplace transform

$$q(p)=\int_0^\infty e^{-pr}\rho(r)r^2\,dr\ , \tag{2.1}$$

where $\rho(r)$ is the vacuum-polarization charge density due to all the diagrams with a single electron loop interacting with a point nucleus of charge Ze ($e=|e|$), including those of Figs. 1(a) and 1(d). They expand their result for $q(p)$ in powers of $Z\alpha$ [Eq. (WK52)],

$$q(p)=\sum_{n=0}^{\infty}(Z\alpha)^{2n+1}q^{(2n+1)}(p)\ , \tag{2.2}$$

and obtain the polarization charge due to the diagram in Fig. 1(d) as the term proportional to $(Z\alpha)^3$. They find [Eqs. (WK50) and (WK54)]

$$(Z\alpha)^3q^{(3)}(p)=-(Z\alpha)^3(e/4\pi^2)\int_{-\infty}^{\infty}\overline{W}^{(3)}(p;y)\,dy\ , \tag{2.3}$$

where $\hbar=c=m=1$, m is the mass of the electron and $-e$ its charge, and $\overline{W}^{(3)}(p;y)$ is given in terms of the functions

$$u=\tfrac{1}{2}p(1+y^2)^{-1/2}\ , \tag{2.4}$$

$$\psi(2,x)=-\int_0^x t^{-1}\ln(1-t)\,dt \tag{2.5a}$$

$$=\sum_{n=1}^{\infty}\frac{x^n}{n^2}\ ,\quad |x|\le 1 \tag{2.5b}$$

$$-2\overline{W}^{(3)}(p;y)=\frac{y^4}{(1+y^2)^{5/2}u^3}\left\{\frac{4}{3}\ln^3(1+u)+2\psi(2,u^2)\ln(1-u)+\frac{2}{3}u^3-\frac{\pi^2}{3}\left[\ln(1-u^2)+u^2\right]\right.$$

$$+2\int_0^u \frac{dx}{x}\ln^2(1-x^2)-2\left[\ln(1-u^2)\ln\frac{1+u}{1-u}+2u^3\right]\ln u\Bigg\}$$
$$+\frac{y^2}{(1+y^2)^{3/2}u^2}\Bigg\{\psi(2,u)\ln\frac{1+u}{1-u}-2u^2-\frac{\pi^2}{6}\left[\ln\frac{1+u}{1-u}-2u\right]+u\ln^2(1+u)+\frac{1}{2}u\psi(2,u^2)$$
$$+\frac{1}{2}\int_0^u \frac{dx}{x}\ln(1-x^2)\ln\frac{1+x}{1-x}-\left[\frac{1}{2}\ln^2\frac{1+u}{1-u}+u\ln\frac{1+u}{1-u}-4u^2\right]\ln u\Bigg\}$$
$$+\frac{y^2}{(1+y^2)^{5/2}u^2(1-u^2)}\Bigg\{2(1-u)\ln^2(1+u)-(1+u)\psi(2,u^2)-u^2(1-u^2)$$
$$+\frac{\pi^2}{3}u^3-2\left[\ln(1-u^2)-u\ln\frac{1+u}{1-u}+3u^2(1-u^2)\right]\ln u\Bigg\}$$
$$+\frac{1}{(1+y^2)^{3/2}u(1-u^2)}\Bigg\{(1-u)\psi(2,u)-(1+3u)\psi(2,-u)-2u(1-u^2)$$
$$-\frac{\pi^2}{6}u^2(1+u)-\left[\ln\frac{1+u}{1-u}+u\ln(1-u^2)-2u(1-u^2)\right]\ln u\Bigg\}\ . \qquad (2.6)$$

Wichmann and Kroll expand this expression for $q^{(3)}(p)$ in powers of $\frac{1}{2}p$, obtaining [Eq. (WK59)]

$$q^{(3)}(p)=\frac{e}{4\pi^2}\left[\frac{\pi}{4}\left(-\frac{5\pi^2}{72}+\frac{13}{24}\right)\frac{p}{2}\right.$$
$$+\left(-\frac{2}{3}\frac{\pi^2}{6}+\frac{19}{15}\right)\left(\frac{p}{2}\right)^2+\frac{\pi}{4}\left(-\frac{31\pi^2}{360}+\frac{1}{2}\right)\left(\frac{p}{2}\right)^3$$
$$\left.+\left(-\frac{16}{135}\ln p-\frac{8\pi^2}{90}+\frac{3347}{2835}\right)\left(\frac{p}{2}\right)^4+O(p^5)\right]\ . \qquad (2.7)$$

This information is useful for obtaining some radial moments of $\rho^{(3)}(r)$, the charge density whose Laplace transform is $(Z\alpha)^3q^{(3)}(p)$, since we have

$$\int_0^\infty r^n[r^2\rho^{(3)}(r)]\,dr=(Z\alpha)^3\left(-\frac{d}{dp}\right)^n q^{(3)}(p)\Big|_{p=0}\ . \qquad (2.8)$$

For $n=0$, we find from Eq. (2.7) that the total polarization charge vanishes, as it must, because it would otherwise change the nuclear charge seen by a distant observer. For $n=4$ in Eq. (2.8), the $\ln p$ term in Eq. (2.7) causes this moment of $\rho^{(3)}(r)$ to diverge, and in fact this term can be used to show that

$$r^2\rho^{(3)}(r)\sim e\frac{(Z\alpha)^3}{4\pi}\left(\frac{40}{225\pi}\right)\frac{1}{r^5} \qquad (2.9)$$

for $r\gg 1$, as Wichmann and Kroll point out in Eq. (WK60).

Wichmann and Kroll also find the limiting value of $q^{(3)}(p)$ when p becomes infinite, given in Eq. (WK61) as

$$\lim_{p\to\infty}q^{(3)}(p)=-\frac{e}{4\pi^2}\left(\frac{\pi^2}{6}-\frac{7}{9}-\frac{2}{3}\zeta(3)\right)\ , \qquad (2.10)$$

where $\zeta(z)$ is the Riemann ζ function. This means that the charge density $\rho^{(3)}(r)$ behaves like a Dirac δ function at the origin,

$$\rho^{(3)}(r)=\delta Q\delta^3(\vec{r})\quad (r\to 0)\ , \qquad (2.11a)$$

with [from Eq. (WK70)]

$$\delta Q=-e\frac{(Z\alpha)^3}{\pi}\left(\frac{\pi^2}{6}-\frac{7}{9}-\frac{2}{3}\zeta(3)\right)$$
$$\approx -e(Z\alpha)^3(0.020940)\ . \qquad (2.11b)$$

Note that δQ is opposite in sign to the nuclear charge. Since the net polarization charge must vanish, the total charge outside the origin must cancel δQ. The asymptotic charge density given in Eq. (2.9) is, in fact, opposite in sign to δQ.

Since muons in the states in which we are interested spend most of their time well within half an electron Compton wavelength from the nucleus, their level shifts due to the polarization charge $\rho^{(3)}(r)$ are approximated by the shifts from the Coulomb potential due to the charge δQ at the origin. However, with the information at hand, rather singular behavior of $\rho^{(3)}(r)$, and its consequent large corrections to the Coulomb potential from δQ, could not be ruled out entirely, so that it was desirable to learn more about $\rho^{(3)}(r)$ near the origin.

III. POLARIZATION CHARGE NEAR NUCLEUS

The large-p behavior of $q^{(3)}(p)$ is determined by how $\rho^{(3)}(r)$ behaves when r is small, and so the integral in Eq. (2.3) was carried out analytically for large p and $q^{(3)}(p)$ was obtained up to terms that vanish faster than $1/p^3$. The evaluation of the integral is discussed in the Appendix. It was found that

$$(Z\alpha)^3q^{(3)}(p)=\frac{\delta Q}{4\pi}+\frac{a}{p^2}-\frac{2c}{p^3}\ln\frac{p}{4}+\frac{2d'}{p^3}$$

$$+O\left(\frac{\ln^m p}{p^4}\right), \quad (3.1)$$

where

$$a=+e\frac{(Z\alpha)^3}{\pi^2}\left(\frac{1}{2}\zeta(2)-3\zeta(3)+\frac{45}{16}\zeta(4)\right) \quad (3.2a)$$

$$\approx+e(Z\alpha)^3(0.026377)\ ,$$

$$c=+e(Z\alpha)^3(1/3\pi)\ , \quad (3.2b)$$

and

$$d'=-e(Z\alpha)^3(1/\pi)[\tfrac{17}{18}-\zeta(3)]\ . \quad (3.2c)$$

This indicates that, for $r\ll 1$,

$$\rho^{(3)}(r)=\delta Q\delta^{(3)}(\vec{r})+a/r+c\ln 4G^{-1}r-d+O(r\ln^m r)\ , \quad (3.3)$$

with

$$G=e^{-\gamma}\ ,$$

$$d=+e(Z\alpha)^3(1/\pi)[\tfrac{13}{9}-\zeta(3)]\ , \quad (3.2d)$$

and γ is Euler's constant, $\gamma\approx 0.5772157$. Note that there is no term linear in $1/p$ in the expansion in Eq. (3.1), and that a in Eq. (3.3) has the same sign as the charge density for large r [Eq. (2.9)].

It is convenient to define a normalized charge density

$$\bar{\rho}(r)\equiv\frac{4\pi}{-\delta Q}\rho^{(3)}(r) \quad (3.4)$$

and to define the quantities

$$\langle r^n\rangle\equiv\int_0^\infty[r^2\bar{\rho}(r)]r^n dr\ , \quad (3.5)$$

whose values, determined from Eqs. (2.7) and (2.8), are

$$\langle 1\rangle=1\ , \quad (3.6a)$$

$$\langle r\rangle\approx 0.85794\ , \quad (3.6b)$$

$$\langle r^2\rangle\approx 1.29242\ , \quad (3.6c)$$

$$\langle r^3\rangle\approx 3.13290\ , \quad (3.6d)$$

where, in evaluating Eq. (3.5) for $n=0$, the contribution from the δ function at $r=0$ has been omitted. Equation (3.6a) thus expresses the condition that the net charge density outside the origin must be exactly $-\delta Q$. It will be convenient, whenever a charge density is mentioned in the remainder of this paper, to assume that the δ function is omitted.

For the transitions of interest here, the average radius of the muon's orbit is typically between 0.2 and 0.4 Compton wavelengths. The approximation given in Eq. (3.3) is not accurate at this distance: the last three terms in Eq. (3.3) begin to be comparable in size for $r\approx 0.1$. It is therefore necessary to employ some sort of interpolation for $\rho^{(3)}(r)$ in order to obtain an estimate of its effect on the muonic states, using the known behavior of $\rho^{(3)}(r)$ for small and large r and the conditions contained in Eq. (2.8) as a guide. To base the calculation on an elaborate interpolation incorporating all the bits of information about $\rho^{(3)}(r)$ does not seem to be justified, because the accuracy of the result is difficult to estimate, and the uncertainty in estimates based on cruder interpolations is still less than the uncertainty in computing the effect of the atomic electrons on the muonic levels. Furthermore, the higher-moment conditions of Eq. (2.8) do not strongly limit the behavior of $\rho^{(3)}(r)$ near the origin, because the moments with the higher powers of r in the integrand are mostly determined by the region where r is comparable with or greater than the Compton wavelength.

Two simple interpolations $\rho_{\rm I}$ and $\rho_{\rm II}$ were therefore tried. Both assumed the small-r and large-r behavior of $\rho^{(3)}(r)$ given in Eqs. (3.3) and (2.9), abruptly terminated at the two radii R_1 and R_2. Expressed in terms of the normalized charge density, it was assumed that, for $r\leq R_1$,

$$r^2\bar{\rho}_{\rm I,\,II}(r)=\bar{a}r+\bar{c}r^2\ln 4G^{-1}r-\bar{d}r^2$$

$$=\bar{a}r+\bar{c}r^2\ln Dr\ , \quad (3.7)$$

with

$$\bar{a}\approx 15.8292\ , \quad (3.8a)$$

$$\bar{c}\approx 63.6739\ , \quad (3.8b)$$

$$\bar{d}\approx 46.3013\ , \quad (3.8c)$$

$$D\approx 3.44301\ , \quad (3.8d)$$

which are obtained from Eqs. (3.2); and for $r\geq R_2$,

$$r^2\bar{\rho}_{\rm I,\,II}(r)=\bar{b}/r^5\ , \quad (3.9)$$

with

$$\bar{b}\approx 2.70241\ , \quad (3.10)$$

which is obtained from Eq. (2.9).

Between R_1 and R_2 the behavior chosen for the interpolations for $r^2\bar{\rho}(r)$ was a constant one for $r^2\bar{\rho}_{\rm I}$ and one quadratic in r for $r^2\bar{\rho}_{\rm II}$. The interpolation was required to be a continuous function of r, so that only one parameter was free to vary in $\rho_{\rm I}$, three in $\rho_{\rm II}$. The interpolations and parameter values are given in Table I. The errors in satisfying the conditions in Eqs. (3.6), defined as

$$\Delta_n=(\langle r^n\rangle_{\rm interp}-\langle r^n\rangle)/\langle r^n\rangle\ , \quad (3.11)$$

are also given. The parameter values given in Table I were chosen by requiring that $\sum_{n=0}^{3}w_n(\Delta_n)^2$ be a minimum, where $w_1=w_2=w_3=0$ for $\rho_{\rm I}$ and $w_3=0$ for $\rho_{\rm II}$, the other weights being chosen to produce as small Δ_1 as possible and still keep Δ_0 near 0.5%.

These interpolations are graphed in Fig. 2, as well as an interpolation that satisfies the condi-

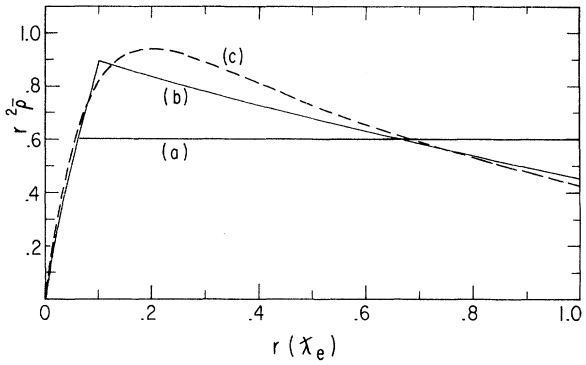

FIG. 2. Interpolations $r^2\bar{\rho}_{\rm I}$ and $r^2\bar{\rho}_{\rm II}$ [curves (a) and (b)] used to estimate the level shifts due to $\rho^{(3)}(r)$. The dashed curve (c) is a more elaborate interpolation that satisfies the conditions (3.6) in the text exactly.

tions in Eqs. (3.6) exactly and has the correct asymptotic behavior for large r of Eq. (3.9), but for small r has the asymptotic behavior of $r^2\bar{\rho}(r)$ only as far as the term linear in r in Eq. (3.7). It is not used in any of the calculations and it did not influence the choice in parameters for the interpolations used, but it is perhaps useful for comparison with the simpler interpolations, since it satisfies all the moment conditions (3.6) exactly and the simpler interpolations do not. The equation for this interpolation is

$$r^2\bar{\rho}(r)=\frac{15.83r}{(1+1.3426r)^6}+\frac{8.819r}{(1+0.8044r)^8}+2.934r^2e^{-2.449r}\ .$$

The number of parameters in the equation equals the number of conditions that the equation was required to satisfy.

The potential produced by the charge density ρ can be written (in Gaussian cgs units) as

$$\phi(r)=4\pi r^{-1}\int_0^r (r'^2-rr')\rho(r')\,dr' \qquad (3.12)$$

when ρ is nicely enough behaved at the origin, as it is here if the δ function is treated separately. Let us do this now.

The level shift due to the point charge given in Eq. (2.11) may be computed by finding the change in the Dirac energy for a point nucleus after the substitution

$$Ze\to Ze+\delta Q\ . \qquad (3.13)$$

In many cases this is given accurately enough by

$$\Delta E_{n,j}=\frac{\partial E_{n,j}}{\partial Z}\,\frac{\delta Q}{e} \qquad (3.14a)$$

$$\approx -\alpha\,\frac{Z\alpha}{n^2}\,\frac{\delta Q}{e}\left[1+\frac{2(Z\alpha)^2}{n}\left(\frac{1}{j+\frac{1}{2}}-\frac{3}{4n}\right)\right]\mu\ , \qquad (3.14b)$$

where μ is the mass of the muon, and n and j the quantum numbers of the atomic state. The relative level shifts that result are listed in the first column of Table II under δQ for the transitions of interest here. For $Z=82$, the substitution (3.13) was made in the exact formula for the Dirac energy and the resulting change in the energy found. It differed from the result of using Eq. (3.14b) by 0.1 eV and is quoted instead in Table II.

Wichmann and Kroll also obtained the Laplace transform of the polarization charge density due to the higher-order diagrams, like the one in Fig. 1(d), but with more interactions between the electron loop and the nuclear charge. The charge densities in all the higher orders were shown to again exhibit a point charge at $r=0$, smaller in each succeeding order, but always with the same sign as in the $(Z\alpha)^3$ order. The point charge $\delta Q'$ due to the $(Z\alpha)^3$ and higher orders is given in Eq. (WK70), and its approximate numerical value given in Eqs. (WK71) and (WK72):

$$\delta Q'\approx\delta Q-e(Z\alpha)^5(0.007121)[1+(Z\alpha)^2(0.5183)]\ . \qquad (3.15)$$

If $\delta Q'$ is used in Eqs. (3.14) instead of δQ, the second column in Table II, under $\delta Q'$, results. Again, the exact difference in energies is quoted rather than the result of Eq. (3.14b) for $Z=82$.

We must now consider the level shifts due to the rest of the polarization charge density with the δ function omitted. These may be obtained from first-order perturbation theory using the potential given in Eq. (3.12). In our calculation, the solutions of the Dirac equation for a point nucleus were used as wave functions for the muon, though

TABLE I. Interpolations used in estimating the level shifts due to the diagram in Fig. 1(d). The Δ_n are the errors in satisfying conditions (3.6).

Interpolation I

$r^2\bar{\rho}_{\rm I}(r)=m,\quad R_1\le r\le R_2$

$R_1=0.061842$
$R_2=1.35020$
$m=0.60223$

$\Delta_0=0$	$\Delta_2=-4.4\%$
$\Delta_1=+6.6\%$	$\Delta_3=-20.2\%$

Interpolation II

$r^2\bar{\rho}_{\rm II}(r)=m-s(r-R_1)+t(r-R_1)(r-R_2),\quad R_1\le r\le R_2$

$R_1=0.098815$
$R_2=3.1115$
$m=0.89383$
$s=0.29362$
$t=0.09252$

$\Delta_0=-0.57\%$	$\Delta_2=-3.4\%$
$\Delta_1=+1.5\%$	$\Delta_3=-13.8\%$

it was scarcely necessary, since even for lead the nonrelativistic wave functions gave a result differing by only 0.1 eV. The expectation value of the potential was found by numerical integration. The relative changes in the levels produced by the interpolations ρ_I and ρ_{II} are listed in the third and fourth columns of Table II under ρ_I and ρ_{II}, respectively.

The level shift due to $\rho^{(3)}$ is probably no further from one of the estimates based on ρ_I and ρ_{II} than the latter are from each other, since it is the charge density for $r \lesssim 0.3$ largely determining the potential for the states of interest here, and within this distance it is not likely that $\rho^{(3)}$ departs very much from the area defined by the two interpolations. Consequently, we will take the shift in the transition energy due to $\rho^{(3)}$ to be the mean value of the estimates from ρ_I and ρ_{II} with an uncertainty equal to 1.5 times the separations between the estimates. The values that result are listed in the fifth column of Table II.

We must still consider the contributions to the level shifts from the higher-order diagrams. We have already used the results of Wichmann and Kroll to determine the shifts produced by the point charge at the origin due to the higher-order diagrams, which are included under $\delta Q'$ in Table II. The shifts due to the polarization charge outside the origin are, of course, rather small, and we shall examine them mostly in the spirit of learning how large an error may be involved in not determining these shifts exactly.

Two facts are known about the polarization charge density outside the origin due to the higher-order diagrams. The first is that the net charge outside the origin must be the negative of the point charge at the origin. The second fact may be obtained from the first term in the expansion for small p of $q^{(5)}(p)$ given by Wichmann and Kroll in Eq. (WK68),

$$\frac{d}{dp} q^{(5)}(p) \approx -\frac{e}{4\pi^2}(0.015191) \ .$$

If we define a normalized charge density as in Eq. (3.4),

$$\bar{\rho}(r) = \frac{4\pi}{-\delta Q^{(5)}} \rho^{(5)}(r) \ ,$$

where $\delta Q^{(5)}$ is the point charge due to the fifth-order diagram, and determine $\langle r \rangle$ for this nor-

TABLE II. Energy shifts from the diagram in Fig. 1(d) and higher orders. The shifts due to the point charge induced at the origin to order $(Z\alpha)^3$ and to all orders are given under δQ and $\delta Q'$, respectively. The shifts produced by the interpolations ρ_I and ρ_{II} are listed under ρ_I and ρ_{II}, respectively. The estimated shifts due to the polarization charge outside the origin to order $(Z\alpha)^3$ and to all orders are given in columns 5 and 6, respectively, and the net shifts due to the diagram in Fig. 1(d) and all higher-order diagrams are given in the last column. All energies are given in eV.

Z	Element	Transition	δQ (eV)	$\delta Q'$ (eV)	ρ_I (eV)	ρ_{II} (eV)	$(Z\alpha)^3$ shift (sans δQ)	$(Z\alpha)^3$ + (higher-orders) shift (sans $\delta Q'$)	Net shift (eV)
20	Ca	$3d_{3/2}$-$2p_{1/2}$	−1.04	−1.05	0.10	0.12	0.11 ± 0.03	0.11 ± 0.03	−0.94 ± 0.03
		$3d_{5/2}$-$2p_{3/2}$	−1.02	−1.03	0.10	0.12	0.11 ± 0.03	0.11 ± 0.03	−0.92 ± 0.03
22	Ti	$3d_{3/2}$-$2p_{1/2}$	−1.53	−1.54	0.13	0.16	0.14 ± 0.05	0.14 ± 0.05	−1.40 ± 0.05
		$3d_{5/2}$-$2p_{3/2}$	−1.50	−1.51	0.13	0.16	0.14 ± 0.05	0.14 ± 0.05	−1.36 ± 0.05
26	Fe	$3d_{3/2}$-$2p_{1/2}$	−3.01	−3.05	0.20	0.25	0.22 ± 0.08	0.23 ± 0.09	−2.82 ± 0.09
		$3d_{5/2}$-$2p_{3/2}$	−2.92	−2.96	0.20	0.25	0.22 ± 0.08	0.23 ± 0.09	−2.74 ± 0.09
38	Sr	$4f_{5/2}$-$3d_{3/2}$	−4.7	−4.9	0.5	0.6	0.6 ± 0.2	0.6 ± 0.2	−4.3 ± 0.2
		$4f_{7/2}$-$3d_{5/2}$	−4.7	−4.8	0.5	0.6	0.6 ± 0.2	0.6 ± 0.2	−4.2 ± 0.2
47	Ag	$4f_{5/2}$-$3d_{3/2}$	−11.2	−11.7	0.9	1.1	1.0 ± 0.3	1.0 ± 0.4	−10.7 ± 0.4
		$4f_{7/2}$-$3d_{5/2}$	−11.0	−11.4	0.9	1.1	1.0 ± 0.3	1.0 ± 0.4	−10.4 ± 0.4
48	Cd	$4f_{5/2}$-$3d_{3/2}$	−12.2	−12.8	0.9	1.2	1.1 ± 0.4	1.1 ± 0.4	−11.7 ± 0.4
		$4f_{7/2}$-$3d_{5/2}$	−11.9	−12.5	0.9	1.2	1.1 ± 0.4	1.1 ± 0.4	−11.4 ± 0.4
50	Sn	$4f_{5/2}$-$3d_{3/2}$	−14.4	−15.1	1.1	1.3	1.2 ± 0.4	1.2 ± 0.4	−13.9 ± 0.4
		$4f_{7/2}$-$3d_{5/2}$	−14.1	−14.8	1.0	1.3	1.2 ± 0.4	1.2 ± 0.4	−13.5 ± 0.4
56	Ba	$4f_{5/2}$-$3d_{3/2}$	−22.9	−24.4	1.4	1.8	1.6 ± 0.5	1.7 ± 0.6	−22.6 ± 0.6
		$4f_{7/2}$-$3d_{5/2}$	−22.2	−23.6	1.4	1.8	1.6 ± 0.5	1.7 ± 0.6	−21.9 ± 0.6
56	Ba	$5g_{7/2}$-$4f_{5/2}$	−10.4	−11.0	1.2	1.6	1.4 ± 0.6	1.5 ± 0.6	−9.5 ± 0.6
		$5g_{9/2}$-$4f_{7/2}$	−10.2	−10.8	1.2	1.6	1.4 ± 0.6	1.5 ± 0.6	−9.3 ± 0.6
82	Pb	$5g_{7/2}$-$4f_{5/2}$	−48.9	−55.9	3.7	4.6	4.2 ± 1.4	4.8 ± 1.8	−51.2 ± 1.8
		$5g_{9/2}$-$4f_{7/2}$	−47.4	−54.3	3.6	4.6	4.1 ± 1.4	4.7 ± 1.8	−49.6 ± 1.8

malized charge density just as we did for $\rho^{(3)}(r)$, using equations analogous to Eqs. (2.8) and (3.5), we find $\langle r\rangle \approx 0.68$ vs 0.86 for $\rho^{(3)}$ [Eq. (3.6b)]. Since these values are not radically different, we may suppose that the charge distribution $\rho^{(5)}(r)$ near the origin behaves somewhat like $\rho^{(3)}(r)$, but is reduced in magnitude by the factor $\delta Q^{(5)}/\delta Q$, since in $\rho^{(5)}(r)$ the net charge outside the origin must cancel $\delta Q^{(5)}$. This assumption permits a simple estimate of the magnitude of the shift due to the higher-order diagrams, since we need only scale down the shifts due to $\rho^{(3)}(r)$ by the appropriate factor: $(\delta Q' - \delta Q)/\delta Q$.

If we add this estimate to the shift due to $\rho^{(3)}(r)$, we obtain the next-to-last column of Table II. We see that even for $Z = 82$ the change in energy is only 0.6 eV. The error in this estimate of the effect of the higher-order diagrams is probably as large as the estimate itself, and in Table II this error has been compounded with the uncertainty already present in the estimate for the shift due to $\rho^{(3)}(r)$.

The estimates of the net effect of the graph in Fig. 1(d) and its higher-order counterparts are given in the last column of Table II. These are seen to differ from the estimates published by Sundaresan and Watson,[4] most significantly for lead, where the difference is about 5 eV. In their approach an interpolation for $q^{(3)}(p)$ was used that for large p deviated from the asymptotic limit as $1/p$ rather than with the $1/p^2$ behavior that has been found here [Eq. (3.1)]. In coordinate space this would mean that $r^2\rho^{(3)}(r)$ does not vanish at $r = 0$, and so with their assumption a greater amount of shielding of the point charge δQ can occur within the muon's orbit, with a correspondingly larger reduction of the energy shift due to the point charge δQ. In general, their interpolation overestimates the effect of the shielding of the point charge by about a factor of 2 for the transitions considered here, and would overestimate more for transitions taking place closer to the nucleus.

IV. DISCUSSION

The most important facts established here are contained in expression (3.3): the sign and magnitude of the polarization charge density near the nucleus due to the diagram in Fig. 1(d). The charge density outside the origin is opposite in sign to the sign of the δ function at the origin [Eq. (2.11)], so that it diminishes rather than augments the potential generated by the δ function; and not by very much, in the cases considered here. The expansion (3.3) becomes more accurate over the region traveled by muons orbiting closer to the nucleus, but the calculation of Wichmann and Kroll from which it is obtained assumes a point nucleus, and when the finite size of the nucleus generates significant corrections to the Dirac value for the energy of the muonic atom, then its modification of the expansion (3.3) must be considered as well. One might hope to approximate the effect of the finite size of the nucleus by assuming that each (infinitesimal) volume element of the nucleus induces a polarization charge proportional to the Wichmann–Kroll result (centered on the volume element) and the nuclear charge contained in the volume element, but it would be difficult to estimate the accuracy of such a procedure.

The discrepancies between the theoretical transition energies, based on the quantum-electrodynamical description of the muonic atoms, and the experimental energies determined by Dixit *et al.*, are still uncomfortably large in four cases. In Table III the energies and discrepancies are listed for the heavier muonic atoms, using the values given by Dixit *et al.*[2] for the theoretical energies and uncertainties, except for the corrections due to the α^2 diagrams in Figs. 1(b) and 1(c), which are taken from Sundaresan and Watson,[4] and the corrections from the higher-order diagrams that have been considered here and are given in the last column of Table II. The experimental energies are quoted from Dixit *et al.*

Most of the radiative corrections to the muonic energy levels have now been checked, and it does not seem likely that any substantial emendations will be forthcoming from that direction.[5] Vogel[6] has reexamined the electron-screening correction and is in agreement with previous calculations.[7,8] If one assumes that nearly all of the electrons are present during the lead $5g$-$4f$ transition, the discrepancy would at best be reduced by about 10 eV for lead, and cascade calculations do not justify this assumption.[6] The corrections due to the finite size and the structure of the nucleus have not been so thoroughly investigated, and perhaps are deserving of more attention. The finite-size corrections are rather large in Ba (-140 eV for $4f_{5/2}$-$3d_{3/2}$ and -53 eV for $4f_{7/2}$-$3d_{5/2}$) and sensitive to the choice for the nuclear shape. For the transitions in lead the finite-size effect is much smaller. The other effects due to the nonideal nature of the nucleus are each estimated to be less than 10 eV in magnitude (except for the correction due to the finite mass of the nucleus, which is mostly accounted for by using the reduced mass of the muon).

It may be important for recent theoretical attempts at a unified theory of weak and electromagnetic interactions[9,10] to establish with confidence the theoretical and experimental transition energies, since the size of the discrepancy provides a useful constraint on some of the theories.[11]

ACKNOWLEDGMENTS

I would like to especially thank Professor Y.

TABLE III. Theoretical and experimental transition energies. The α^2 shifts due to the diagrams in Figs. 1(b) and 1(c) are taken from Ref. 4, the experimental energies from Ref. 2.

Z	Element	Transition	α^2 shift (keV)	$(Z\alpha)^3$ + (higher-orders) shift (keV)	E_{theor} (keV)	E_{expt} (keV)	Discrepancy (eV)
47	Ag	$4f_{5/2}$-$3d_{3/2}$	0.0142	−0.0107	308.458 ± 0.005	308.428 ± 0.019	30 ± 20
		$4f_{7/2}$-$3d_{5/2}$	0.0137	−0.0104	304.780 ± 0.005	304.759 ± 0.017	21 ± 18
48	Cd	$4f_{5/2}$-$3d_{3/2}$	0.0151	−0.0117	321.996 ± 0.005	321.973 ± 0.018	23 ± 19
		$4f_{7/2}$-$3d_{5/2}$	0.0144	−0.0114	317.990 ± 0.005	317.977 ± 0.017	13 ± 18
50	Sn	$4f_{5/2}$-$3d_{3/2}$	0.0169	−0.0139	349.981 ± 0.006	349.953 ± 0.020	28 ± 21
		$4f_{7/2}$-$3d_{5/2}$	0.0163	−0.0135	345.257 ± 0.005	345.226 ± 0.018	31 ± 19
56	Ba	$4f_{5/2}$-$3d_{3/2}$	0.0235	−0.0226	441.366 ± 0.007	441.299 ± 0.021	67 ± 22
		$4f_{7/2}$-$3d_{5/2}$	0.0223	−0.0219	433.910 ± 0.007	433.829 ± 0.019	81 ± 20
56	Ba	$5g_{7/2}$-$4f_{5/2}$	0.0065	−0.0095	201.279 ± 0.004	201.260 ± 0.016	19 ± 16
		$5g_{9/2}$-$4f_{7/2}$	0.0065	−0.0093	199.912 ± 0.004	199.902 ± 0.015	10 ± 16
82	Pb	$5g_{7/2}$-$4f_{5/2}$	0.0202	−0.0512	437.756 ± 0.010	437.687 ± 0.020	69 ± 22
		$5g_{9/2}$-$4f_{7/2}$	0.0194	−0.0496	431.342 ± 0.009	431.285 ± 0.017	57 ± 19

Nambu for many, many informative, enjoyable discussions, and for his generous guidance and support. I would also like to thank Professor H. L. Anderson for his encouragement and helpful comments and information, and Dr. Stanley Brodsky for numerous useful discussions while I was a guest at the Stanford Linear Accelerator Center, where this work was begun and whose hospitality then is very much appreciated.

APPENDIX: DETAILS OF CALCULATION

In order to carry out the integral in Eq. (2.3) for large p, it was first noticed that the integrand given in Eq. (2.6) is even in the integration variable y, so that

$$\int_{-\infty}^{\infty} \bar{W}^{(3)}(p;y)\,dy = \int_0^{\infty} 2\,\bar{W}^{3)}(p;y)\,dy \quad . \tag{A1}$$

Using the definition in Eq. (2.4), the integration variable is changed to u, so that, with $P=\frac{1}{2}p$,

$$\int_{-\infty}^{\infty} \bar{W}^{(3)}(p;y)\,dy = \int_0^P 2\bar{W}^{(3)}(p;y)P(1-u^2/P^2)u^{-2}\,du \quad . \tag{A2}$$

It is perhaps easiest to indicate the succeeding steps in the approach with a specific example, and so the integral of the first term of $\bar{W}^{(3)}$ in (2.6) will be examined. Then we require the behavior for large P of the integral

$$\int_\epsilon^P (1-u^2/P^2)^{3/2}\ln^3(1+u)u^{-4}\,du \quad , \tag{A3}$$

where we have replaced the lower limit by $\epsilon>0$ with the intention of letting it approach zero later; the logarithmic divergence in ϵ is canceled by the next two terms in $\bar{W}^{(3)}$ and is not of any significance. The integral (A3) is then written as

$$\int_\epsilon^P \frac{du}{u^4}\left[\left(1-\frac{3}{2}\frac{u^2}{P^2}\right)\ln^3(1+u) + \left(1-\frac{u^2}{P^2}\right)^{3/2} - 1 + \frac{3}{2}\frac{u^2}{P^2}\right]\ln^3(1+u) \quad . \tag{A4}$$

The first integral may be rewritten as

$$\int_\epsilon^P \frac{du}{u^4}\left(1-\frac{3}{2}\frac{u^2}{P^2}\right)\ln^3(1+u) - \int_P^\infty \frac{du}{u^4}\left(1-\frac{3}{2}\frac{u^2}{P^2}\right)\ln^3(1+u) \quad . \tag{A5}$$

The first integral of (A5) is already in the form we seek, and we need only evaluate some definite integrals to obtain the coefficients due to this term in the expansion of $q^{(3)}(p)$ in powers of $1/P$. The leading behavior of the second integral in (A5) is already of order $(\ln^3 p)/p^3$, and so only the asymptotic behavior of the integrand is required for our purposes. One finds that this is the case in all the analogous terms of $\bar{W}^{(3)}$ involving logarithmic functions, and it is easier to find the asymptotic behavior of all these terms in the first pair of curly brackets in $\bar{W}^{(3)}$ as a whole, because many cancellations take place—in particular, the one under consideration here is canceled.

The second integral in (A4) must still be examined. Though one may handle it directly, the treatment of the integral is easier if it is broken into two parts, as

$$\int_\epsilon^P = \int_\epsilon^s + \int_s^P \quad , \tag{A6}$$

where we choose $s=P^{1/2+\epsilon'}$, $\epsilon'>0$ and small. In the first domain the integral can be shown to fall

faster than $1/P^3$ as $P \to \infty$ by expanding the factor $(1-u^2/P^2)^{3/2}$ in a Taylor series. In the second domain only the asymptotic behavior of $\ln^3(1+u)$ is needed to obtain the contribution that does not fall faster than $1/P^3$. The same situation occurred in the second integral of (A5), and again analogous terms in the first pair of curly brackets of $\bar{W}^{(3)}$ cancel the asymptotic behavior of this term and no integrals need be evaluated.

Much the same approach may be used for the other terms of $\bar{W}^{(3)}$. The terms in $\bar{W}^{(3)}$ that do not involve logarithmic functions can usually be done exactly and considered separately. Treatment of the terms involving logarithms is often simplified by integrations by parts and by treating groups of terms together.

The definite integrals required to verify the calculation of Wichmann and Kroll of the asymptotic limit of $q^{(3)}(p)$, such as the first one met in the first term of (A4), include most of those needed for the next terms in the expansion of $q^{(3)}(p)$. Contour-integration methods may be used to relate integrals evaluated by other methods and permit a large amount of cross checking in the calculation.

---

*Supported in part by the U. S. Atomic Energy Commission under Contract No. AEC AT (11-1)-264, and the National Science Foundation under Contract No. NSF GP 32904 X.

†Submitted to the Department of Physics, the University of Chicago, in partial fulfillment of the requirements for the Ph.D. degree.

‡Permanent address: Laboratory of Nuclear Studies, Cornell University, Ithaca, N. Y. 14850.

[1]See, for example, the review by Martin L. Perl, Stanford Linear Accelerator Center Publication No. 982, 1971 (unpublished).

[2]M. S. Dixit, H. L. Anderson, C. K. Hargrove, R. J. McKee, D. Kessler, H. Mes, and A. C. Thompson, Phys. Rev. Lett. **27**, 878 (1971). Similar experimental results have since been reported for muonic Hg and Tl. See H. K. Walter *et al.*, Phys. Lett. B **40**, 197 (1972).

[3]E. H. Wichmann and N. M. Kroll, Phys. Rev. **101**, 843 (1956).

[4]M. K. Sundaresan and P. J. S. Watson, Phys. Rev. Lett. **29**, 15 (1972).

[5]One has nevertheless occurred, during the preparation of this manuscript for publication. I am grateful to Dr. N. M. Kroll for bringing to my attention a recent report of work prior to publication by J. Blomqvist, Research Institute for Physics, Stockholm, Sweden. Blomqvist points out that, in the calculation of the α^2 vacuum-polarization correction, the effect of the diagram in Fig. 1(b) has been added twice, because the formula used to calculate the effect of the diagrams in Figs. 1(c) is derived with the contribution from the diagram in Fig. 1(b) included as well, and it need not be added separately. Sundaresan and Watson (Ref. 4) fortunately give separately the effect of the diagram 1(b), and so we may readily correct their values, which we have quoted for the α^2 vacuum-polarization effect in Table III, by reducing them by the amount given for diagram 1(b). One finds that the α^2 effect (and the theoretical transition energies) should be reduced, to correct for the double counting, by 3.7, 3.5; 3.9, 3.7; 4.4, 4.3; 6.5, 6.1; 1.3, 1.4; 5.1, 4.9 eV, reading from top to bottom in Table III. Moreover, Blomqvist indicates that the relativistic correction for the motion of the nucleus has been added with the wrong sign in the theoretical transition energies published by Dixit *et al.* (B. Fricke, J. T. Waber, and V. L. Telegdi have also noted this in a recent report of work prior to publication.) If this error is taken into account, the theoretical energies are now increased back to within a few electron volts of the values listed in Table III. Blomqvist has also investigated, in a very nice way, the behavior near the nucleus of the potential due to the diagram in Fig. 1(d), obtaining an integral representation for the potential in coordinate space and expanding it for small r. Considering the length of these calculations, it is very gratifying to find that our results agree in every respect where comparison is possible. *Footnote added in proof.* Blomqvist's work may be found in Nucl. Phys. B **48**, 95 (1972).

[6]P. Vogel, Caltech Report No. CALT-63-175, 1972 (unpublished).

[7]H. L. Anderson, in *Proceedings of the Third International Conference on High-Energy Physics and Nuclear Structure,* edited by S. Devons (Plenum, New York, 1970), p. 640.

[8]B. Fricke, Nuovo Cimento Lett. **2**, 859 (1969).

[9]S. Weinberg, Phys. Rev. Lett. **19**, 1264 (1967).

[10]H. Georgi and S. L. Glashow, Phys. Rev. Lett. **28**, 1494 (1972).

[11]J. R. Primack and H. R. Quinn, Phys. Rev. D **6**, 3171 (1972).